

# Production and polarization of $S$ -wave quarkonium in potential non-relativistic QCD

Xiang-Peng Wang

Nora Brambilla, Hee Sok Chung & Antonio Vairo

PRD 105 (2022) 11, L111503 & paper in preparation

9<sup>th</sup> International Conference of Quarks & Nuclear Physics

8<sup>th</sup> September 2022

# Outlines

NRQCD factorization for quarkonium production

NRQCD LDMEs in pNRQCD

Fitting production data & polarization predictions

More tests from other observables

Summary & conclusions

## NRQCD factorization for $S$ -wave quarkonium production

- In the framework of NRQCD factorization ([Bodwin, Braaten & Lepage, PRD 51, 1125 \(1995\)](#)), at relative order  $v^4$ , the inclusive cross section of a spin-1  $S$ -wave quarkonium  $V$  is given by

$$\sigma_{V+X} = \hat{\sigma}_{3S_1^{[1]}} \langle \mathcal{O}^V(^3S_1^{[1]}) \rangle + \hat{\sigma}_{3S_1^{[8]}} \langle \mathcal{O}^V(^3S_1^{[8]}) \rangle \\ + \hat{\sigma}_{1S_0^{[8]}} \langle \mathcal{O}^V(^1S_0^{[8]}) \rangle + \sum_{J=0,1,2} \hat{\sigma}_{3P_J^{[8]}} \langle \mathcal{O}^V(^3P_J^{[8]}) \rangle. \quad (1)$$

- $\hat{\sigma}_n$  are the short-distance-coefficients (SDCs), which can be calculated perturbatively,
- $\langle \mathcal{O}^V(^3S_1^{[1]}) \rangle, \langle \mathcal{O}^V(^3S_1^{[8]}) \rangle, \langle \mathcal{O}^V(^1S_0^{[8]}) \rangle, \langle \mathcal{O}^V(^3P_J^{[8]}) \rangle$  are long-distance-matrix-elements (LDMEs), which are non-perturbative, universal and have definite  $v$  scalings.
- NRQCD factorization formalism for  $p_T$ -differential cross section is expected to be valid up to relative order of  $m^2/p_T^2$ .  
[Nayak, Qiu & Sterman, PLB 613, 45 \(2005\); PRD 72, 114012 \(2005\); PRD 74, 074007 \(2006\); Kang \*et al.\* PRD 90, 034006 \(2014\).](#)

## Definitions of the NRQCD LDMEs

The definitions of the previously mentioned LDMEs are

$$\langle \mathcal{O}^V(^3S_1^{[1]}) \rangle = \langle \Omega | \chi^\dagger \sigma^i \psi \mathcal{P}_{V(P=0)} \psi^\dagger \sigma^i \chi | \Omega \rangle, \quad (2a)$$

$$\langle \mathcal{O}^V(^3S_1^{[8]}) \rangle = \langle \Omega | \chi^\dagger \sigma^i T^a \psi \Phi_\ell^{\dagger ab} \mathcal{P}_{V(P=0)} \Phi_\ell^{bc} \psi^\dagger \sigma^i T^c \chi | \Omega \rangle, \quad (2b)$$

$$\langle \mathcal{O}^V(^1S_0^{[8]}) \rangle = \langle \Omega | \chi^\dagger T^a \psi \Phi_\ell^{\dagger ab} \mathcal{P}_{V(P=0)} \Phi_\ell^{bc} \psi^\dagger T^c \chi | \Omega \rangle, \quad (2c)$$

$$\begin{aligned} \langle \mathcal{O}^V(^3P_0^{[8]}) \rangle &= \frac{1}{3} \langle \Omega | \chi^\dagger \left( -\frac{i}{2} \overleftrightarrow{\mathbf{D}} \cdot \boldsymbol{\sigma} \right) T^a \psi \Phi_\ell^{\dagger ab} \mathcal{P}_{V(P=0)} \\ &\quad \times \Phi_\ell^{bc} \psi^\dagger \left( -\frac{i}{2} \overleftrightarrow{\mathbf{D}} \cdot \boldsymbol{\sigma} \right) T^c \chi | \Omega \rangle, \end{aligned} \quad (2d)$$

here the operator  $\mathcal{P}_{\mathcal{Q}(P)} = \sum_X |\mathcal{Q} + X\rangle \langle \mathcal{Q} + X|$  projects onto a state consisting of a quarkonium  $\mathcal{Q}$  with momentum  $P$ ,  $\Phi_\ell = P \exp[-ig \int_0^\infty d\lambda \ell \cdot A^{\text{adj}}(\ell\lambda)]$  is the path-ordered Wilson line along the spacetime direction  $\ell$ , which ensures the gauge invariance.

- It is unclear how to calculate the CO LDMEs from first principle such as lattice, so the CO LDMEs are usually determined through fitting with experimental data.

# Current status of the existing fittings for the $J/\psi$ LDMEs

	$\langle \mathcal{O}^{J/\psi}(^3S_1^{[8]}) \rangle$	$\langle \mathcal{O}^{J/\psi}(^1S_0^{[8]}) \rangle$	$\langle \mathcal{O}^{J/\psi}(^3P_0^{[8]}) \rangle / m^2$
Hamburg	$0.168 \pm 0.046$	$3.04 \pm 0.35$	$-0.404 \pm 0.072$
ANL	$-0.713 \pm 0.364$	$11 \pm 1.4$	$-0.312 \pm 0.151$
IHEP	$0.117 \pm 0.058$	$5.66 \pm 0.47$	$0.054 \pm 0.005$
PKU set 1	0.05	7.4	0
PKU set 2	1.11	0	1.89

**Table:** Selected fittings for the  $J/\psi$  CO LDMEs in units of  $10^{-2} \text{ GeV}^3$ .

- All the fittings are based on NLO calculations.
- The SDCs at large  $p_T$  of P-wave channels are negative at NLO.

## More about existing fittings

- Hamburg ([Butenschön & Kniehl, PRD 84, 051501 \(2011\)](#)): World data fitting with  $p_T > 3\text{Gev}$  including  $e^-p$  collision data, contradicts with polarization measurements.
- ANL ([Bodwin \*et al.\*, PRD 93, 034041 \(2016\)](#)): Combine leading log re-summation from LP fragmentation with NLO fixed order calculation and fit with hadron production data with  $p_T > 10\text{Gev}$ .
- IHEP ([Feng \*et al.\*, PRD 99, 014044 \(2019\)](#)): fit both  $J/\psi$  hadron production and polarization data with  $p_T > 7\text{Gev}$ .
- PKU ([Ma, Wang & Chao, PRL 106, 042002 \(2011\)](#)): fit with  $p_T > 7\text{Gev}$ , the values listed in the table are boundary values, only two combinations are extracted.
- All the existing fittings for the three CO LDMEs are rather sensitive to the choices of data sets and fitting strategies (even the sign can change). Only two linear combinations are well constrained with large  $p_T$  data.

## Two scenarios

The current situation of spin-1  $S$ -wave quarkonium production at hadron colliders can be summarized as

- $^1S_0^{[8]}$  dominance: naturally gives almost un-polarized predictions.
- The bulk of the cross section comes from the remnant of the cancellation between  $^3S_1^{[8]}$  and  $^3P_J^{[8]}$  channels.
- Any linear combination of the above scenarios are allowed.
- The fit in the framework of NRQCD factorization cannot support or rule out  $^1S_0^{[8]}$  dominance because there are 3 color-octet LDMEs but only 2  $p_T$  scalings from the SDCs ( $1/p_T^4$  and  $1/p_T^6$ ).

## pNRQCD in strong coupled region

- Potential NRQCD (pNRQCD) (Pineda & Soto, NPB 64, 428 (1998); Brambilla *et al.*, NPB 566, 275 (2000), RMP 77, 1423 (2005)) follows from NRQCD by integrating out the modes associated with scales larger than  $mv^2$ .
- The strong coupled region, in which  $\Lambda_{QCD} \gg mv^2$ , is fulfilled by non Coulombic quarkonium states such as  $J/\psi, \psi(2S)$  and excited  $\Upsilon$  states. The degree of freedom is the singlet field  $S(x_1, x_2)$ , which describes the  $Q\bar{Q}$  in a color-singlet state.
- In the strong coupled region, the NRQCD LDMEs can be expressed in terms of wave-functions at the origin and universal gluonic correlators, which significantly reduces the number of independent LDMEs.  
Brambilla *et al.*, PRL 88, 012003 (2002), PRD 67, 034018 (2003);  
Brambilla *et al.*, JHEP 04 (2020) 095;  
Brambilla, Chung & Vairo, PRL 126, 082003 (2021), JHEP 09 (2021) 032.

# NRQCD LDMEs in pNRQCD

In the strong coupled region, at leading order in quantum mechanic perturbation theory, we have (neglect corrections of order  $1/N_c^2$ )

$$\langle \mathcal{O}^V(^3S_1^{[1]}) \rangle = 2N_c \times \frac{3|R_V^{(0)}(0)|^2}{4\pi}, \quad (3a)$$

$$\langle \mathcal{O}^V(^3S_1^{[8]}) \rangle = \frac{1}{2N_cm^2} \frac{3|R_V^{(0)}(0)|^2}{4\pi} \mathcal{E}_{10;10}, \quad (3b)$$

$$\langle \mathcal{O}^V(^1S_0^{[8]}) \rangle = \frac{1}{6N_cm^2} \frac{3|R_V^{(0)}(0)|^2}{4\pi} c_F^2 \mathcal{B}_{00}, \quad (3c)$$

$$\langle \mathcal{O}^V(^3P_0^{[8]}) \rangle = \frac{1}{18N_c} \frac{3|R_V^{(0)}(0)|^2}{4\pi} \mathcal{E}_{00}, \quad (3d)$$

where  $c_F = 1 + \frac{\alpha_s}{2\pi} [C_F + C_A(1 + \log \Lambda/m)] + O(\alpha_s^2)$  in the  $\overline{\text{MS}}$  scheme at the scale  $\Lambda$ ,  $R_V^{(0)}(0)$  is the wave-function at the origin,  $\mathcal{E}_{10;10}$ ,  $\mathcal{B}_{00}$ , and  $\mathcal{E}_{00}$  are universal gluonic correlators of dimension 2 defined by:

## Gluonic correlators

$$\begin{aligned} \mathcal{E}_{10;10} = & \left| d^{dac} \int_0^\infty dt_1 t_1 \int_{t_1}^\infty dt_2 g E^{b,i}(t_2) \right. \\ & \left. \times \Phi_0^{bc}(t_1; t_2) g E^{a,i}(t_1) \Phi_0^{df}(0; t_1) \Phi_\ell^{ef} |\Omega\rangle \right|^2, \end{aligned} \quad (4a)$$

$$\mathcal{B}_{00} = \left| \int_0^\infty dt g B^{a,i}(t) \Phi_0^{ac}(0; t) \Phi_\ell^{bc} |\Omega\rangle \right|^2, \quad (4b)$$

$$\mathcal{E}_{00} = \left| \int_0^\infty dt g E^{a,i}(t) \Phi_0^{ac}(0; t) \Phi_\ell^{bc} |\Omega\rangle \right|^2, \quad (4c)$$

where  $\Phi_0(t, t') = \mathcal{P} \exp[-ig \int_t^{t'} d\tau A_0^{\text{adj}}(\tau, \mathbf{0})]$  is a Schwinger line.

- Note that the above correlators are not positive definite in dimensional regularization since the power divergences are automatically subtracted.

pNRQCD predicts  $\frac{\sigma_{\psi(2S)}^{\text{direct}}}{\sigma_{J/\psi}^{\text{direct}}} \simeq \frac{|R_{2S}(0)|^2}{|R_{1S}(0)|^2}$

- At large  $p_T$ , the prompt cross section ratio measured by CMS is

$$\frac{\sigma_{\psi(2S)}^{\text{prompt}}}{\sigma_{J/\psi}^{\text{prompt}}} \times \frac{\text{Br}(\psi(2S) \rightarrow \mu^+ \mu^-)}{\text{Br}(J/\psi \rightarrow \mu^+ \mu^-)} \simeq 0.044. \quad (5)$$

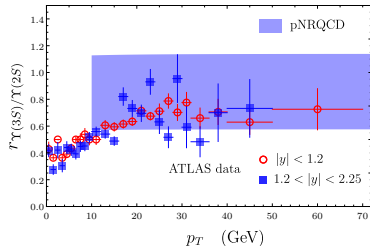
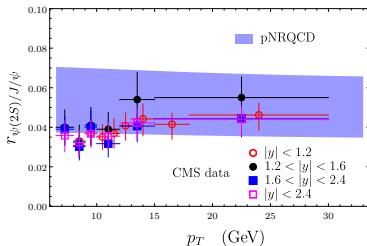
- $\text{Br}(\psi(2S) \rightarrow J/\psi + X) = 0.614$ ,  $\text{Br}(\psi(2S) \rightarrow \mu^+ \mu^-) = 0.793\%$ ,  $\text{Br}(J/\psi \rightarrow \mu^+ \mu^-) = 5.971\%$ , the feeddown from  $\psi(2S)$  to  $J/\psi$  is about 0.2. The feeddown from  $\chi_{cJ}$  to  $J/\psi$  is about 0.27 at large  $p_T$ .

This gives

$$\frac{\sigma_{\psi(2S)}^{\text{direct}}}{\sigma_{J/\psi}^{\text{direct}}} \simeq \frac{0.044 \times 5.971\% / 0.793\%}{1 - 0.2 - 0.27} = 0.63, \quad (6)$$

$$\frac{|R_{2S}(0)|^2}{|R_{1S}(0)|^2} = \frac{m_{\psi(2S)}^2 \Gamma(\psi(2S) \rightarrow \mu^+ \mu^-)}{m_{J/\psi}^2 \Gamma(J/\psi \rightarrow \mu^+ \mu^-)} = \frac{3.6861^2 \times 2.33}{3.0969^2 \times 5.33} = 0.60. \quad (7)$$

# Cross section ratios in pNRQCD



$$r_{\psi(2S)/J/\psi} = \frac{B_{\psi(2S) \rightarrow \mu^+ \mu^-} \sigma_{\psi(2S)}^{\text{prompt}}}{B_{J/\psi \rightarrow \mu^+ \mu^-} \sigma_{J/\psi}^{\text{prompt}}}, \quad (8)$$

$$r_{\Upsilon(3S)/\Upsilon(2S)} = \frac{B_{\Upsilon(3S) \rightarrow \mu^+ \mu^-} \times \sigma_{\Upsilon(3S)}^{\text{inclusive}}}{B_{\Upsilon(2S) \rightarrow \mu^+ \mu^-} \times \sigma_{\Upsilon(2S)}^{\text{inclusive}}} \quad (9)$$

## Evolution of $\mathcal{B}_{00}$

$\mathcal{B}_{00}$  has the scale dependence at one-loop in a way that  $c_F^2 \mathcal{B}_{00}$  is scale invariant at one-loop level.

With  $c_F = 1 + \frac{\alpha_s}{2\pi} [C_F + C_A(1 + \log \Lambda/m)] + \mathcal{O}(\alpha_s^2)$ , we have

$$\frac{d\mathcal{B}_{00}(\mu)}{d\log(\mu)} = \mathcal{B}_{00}(\mu) \left[ -\frac{\alpha_s}{\pi} + \mathcal{O}(\alpha_s^2) \right], \quad (10)$$

which leads to the RG-improved evolution expression

$$\mathcal{B}_{00}(m_b) = \mathcal{B}_{00}(m_c) \left( \frac{\alpha_s(m_b)}{\alpha_s(m_c)} \right)^{\frac{2C_A}{\beta_0}} = 0.774 \times \mathcal{B}_{00}(m_c), \quad (11)$$

with  $\beta_0 = \frac{11}{3}C_A - \frac{2}{3}n_f$ ,  $n_f = 4$ ,  $m_c = 1.5\text{Gev}$ ,  $m_b = 4.75\text{Gev}$ .

- The evolution of  $\mathcal{B}_{00}$  is numerical small.

## Evolution of $\mathcal{E}_{10;10}$

At one-loop, we have

$$\mathcal{E}_{10;10}|_{\text{UV}}^{\text{one-loop}} = \frac{2\alpha_s}{3\pi} \frac{N_c^2 - 4}{N_c} \log(\mu) \mathcal{E}_{00}, \quad (12)$$

which implies the scale dependence of  $\mathcal{E}_{10;10}$ . The RG-improved evolution expression is

$$\begin{aligned} \mathcal{E}_{10;10}(m_b) &= \mathcal{E}_{10;10}(m_c) + \frac{4}{3} \frac{1}{\beta_0} \frac{N_c^2 - 4}{N_c} \mathcal{E}_{00} \log \frac{\alpha_s(m_c)}{\alpha_s(m_b)} \\ &\simeq \mathcal{E}_{10;10}(m_c) + 0.1 \mathcal{E}_{00}. \end{aligned} \quad (13)$$

Note that the above evolution equation also indicates the well-known evolution of the NRQCD LDMEs

$$\frac{d}{d \log \Lambda} \langle \mathcal{O}^V(^3S_1^{[8]}) \rangle = \frac{6(N_c^2 - 4)}{N_c m^2} \frac{\alpha_s}{\pi} \langle \mathcal{O}^V(^3P_0^{[8]}) \rangle. \quad (14)$$

- The evolution of  $\mathcal{E}_{10;10}$  depends on  $\mathcal{E}_{00}$ . This has important implications as we will see later.

## Implications of the evolution of $\mathcal{E}_{10;10}$

- At large  $p_T$ , the following combinations are usually well constrained because of the large  $p_T$  behavior of the SDCs

$$\begin{aligned} M_0^{\psi(nS)} &= \langle \mathcal{O}^{\psi(nS)}(^1S_0^{[8]}) \rangle + 3.9 \langle \mathcal{O}^{\psi(nS)}(^3P_0^{[8]}) \rangle / m_c^2, \\ M_1^{\psi(nS)} &= \langle \mathcal{O}^{\psi(nS)}(^3S_1^{[8]}) \rangle - 0.56 \langle \mathcal{O}^{\psi(nS)}(^3P_0^{[8]}) \rangle / m_c^2, \end{aligned} \quad (15)$$

Ma, Wang & Chao, PRL 106, 042002 (2011),

$$\begin{aligned} M_0^{\Upsilon(nS)} &= \langle \mathcal{O}^{\Upsilon(nS)}(^1S_0^{[8]}) \rangle + 3.8 \langle \mathcal{O}^{\Upsilon(nS)}(^3P_0^{[8]}) \rangle / m_b^2, \\ M_1^{\Upsilon(nS)} &= \langle \mathcal{O}^{\Upsilon(nS)}(^3S_1^{[8]}) \rangle - 0.52 \langle \mathcal{O}^{\Upsilon(nS)}(^3P_0^{[8]}) \rangle / m_b^2. \end{aligned} \quad (16)$$

Han *et al.* PRD 94, 014028 (2016).

- The evolution makes it possible to determine the three correlators with both charmonium and bottomonium hadron production data: 3 correlators in 4 (3) independent linear equations. Thanks to the evolution and universality of the correlators.

## Fitting strategies

- We use the measured prompt cross section data at the LHC:  
 $J/\psi, \psi(2S)$ : [Chatrchyan \*et al.\* \(CMS\), JHEP 02, 011 \(2012\)](#),  
[Khachatryan \*et al.\* \(CMS\), PRL 114, 191802 \(2015\)](#)  
 $\Upsilon(2S), \Upsilon(3S)$ : [Aad \*et al.\* \(ATLAS\), PRD 87, 052004 \(2013\)](#).
- We consider the feed-down fractions from  $P$ -wave quarkonia by using the measured feed-down fractions ([Aad \*et al.\* \(ATLAS\), JHEP 07, 154 \(2014\)](#) & [Aaij \*et al.\* \(LHCb\), EPJC 74, 3092 \(2014\)](#)),
- The feed-down fractions from the decays of  $\psi(2S) \rightarrow J/\psi + X$  and  $\Upsilon(3S) \rightarrow \Upsilon(2S) + X$  are given by the PDG.
- The NLO theory predictions are computed using the FDCHQHP package ([Wan & Wang, Comput. Phys. Commun 185, 2939 \(2014\)](#)).
- Instead of fitting 12 color-octet LDMEs for  $J/\psi, \psi(2S), \Upsilon(2S), \Upsilon(3S)$ , we only need to fit three gluonic correlators  $\mathcal{E}_{10;10}, c_F^2 \mathcal{B}_{00}, \mathcal{E}_{00}$  at the scale  $\Lambda = m_c$ , whose values at the scale  $\Lambda = m_b$  are obtained through evolution.

## Fitting strategies and parameter settings

- We obtain the wave-functions at origin through comparing the measured leptonic decays rates ([Ablikim \*et al.\* \(BESIII\), PRD 85, 112008 \(2012\)](#)) with the pNRQCD results at LO in  $v$  and NLO in  $\alpha_s$  ([Brambilla \*et al.\* JHEP 04, 095 \(2020\)](#)), which gives

$$|R_{J/\psi}^{(0)}(0)|^2 = 0.825 \text{ GeV}^3, \quad |R_{\psi(2S)}^{(0)}(0)|^2 = 0.492 \text{ GeV}^3, \\ |R_{\Upsilon(2S)}^{(0)}(0)|^2 = 3.46 \text{ GeV}^3, \quad |R_{\Upsilon(3S)}^{(0)}(0)|^2 = 2.67 \text{ GeV}^3.$$

- The QCD renormalization scale and the scale for the PDF is set to be  $\sqrt{p_T^2 + 4m^2}$ , the NRQCD scales are set to be  $\Lambda = m$  with  $m_c = 1.5\text{Gev}$ ,  $m_b = 4.75\text{Gev}$ ,
- We take the theory uncertainties to be 30% and 10% of the central values for charmonium and bottomonium, respectively, which account for uncalculated corrections of higher order in  $v^2$ .

# Least square fitting results

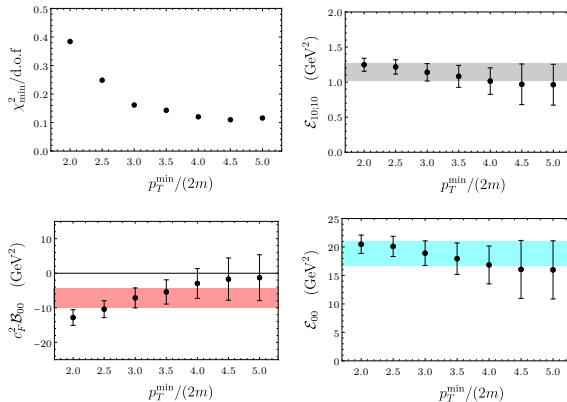


**Figure:** Dependences on the lower  $p_T$  cut  $p_T^{\min}$  of the  $\chi^2_{\min}/\text{d.o.f.}$ , and the values of  $\mathcal{E}_{10;10}$ ,  $c_F^2 \mathcal{B}_{00}$ , and  $\mathcal{E}_{00}$  determined from fits to cross section data. The bands represent the results of the fit for  $p_T^{\min}/(2m) = 3$ .

# Least square fitting results – lower $p_T$ cut dependences

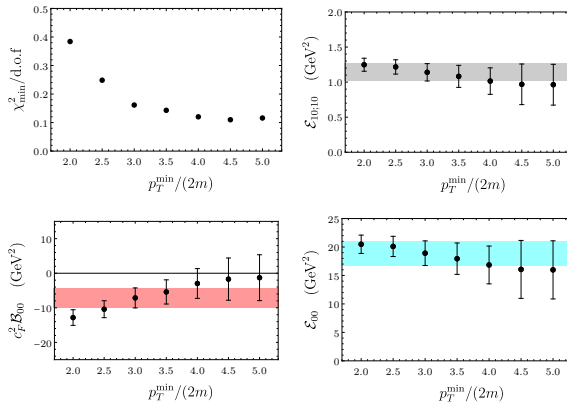


**Figure:** Dependences on the lower  $p_T$  cut  $p_T^{\min}$  of the  $\chi^2_{\min}/\text{d.o.f.}$ , and the values of  $\mathcal{E}_{10;10}$ ,  $c_F^2 \mathcal{B}_{00}$ , and  $\mathcal{E}_{00}$  determined from fits to cross section data. The bands represent the results of the fit for  $p_T^{\min}/(2m) = 3$ .

# Least square fitting results – upper $p_T$ cut dependences

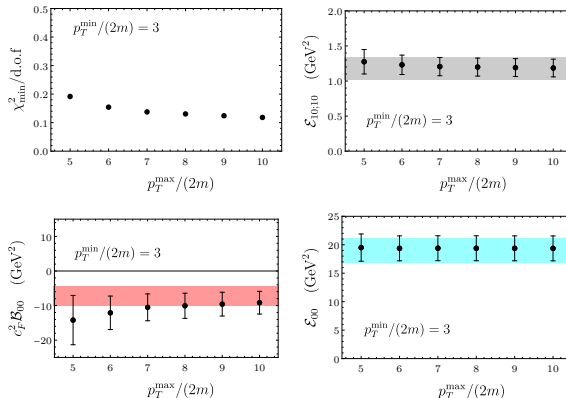


**Figure:** Dependence on the upper  $p_T$  cut  $p_T^{\max}$  with fixed  $p_T^{\min}/(2m) = 3$ . The bands represent the results of the fit for  $p_T^{\min}/(2m) = 3$  with no upper  $p_T$  cut.

# Least square fitting results – upper $p_T$ cut dependences

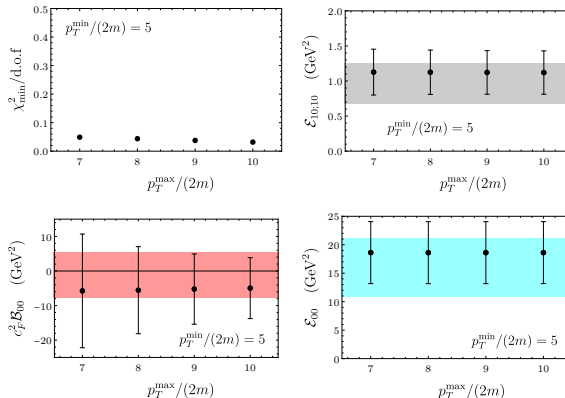


**Figure:** Dependence on the upper  $p_T$  cut  $p_T^{\max}$  with fixed  $p_T^{\min}/(2m) = 5$ . The bands represent the results of the fit for  $p_T^{\min}/(2m) = 5$  with no upper  $p_T$  cut.

## Least square fitting results – updated

$p_T$ region	$\mathcal{E}_{10;10}$ (GeV <sup>2</sup> )	$c_F^2 \mathcal{B}_{00}$ (GeV <sup>2</sup> )	$\mathcal{E}_{00}$ (GeV <sup>2</sup> )
$p_T/(2m) > 3$	$1.14 \pm 0.12$	$-7.13 \pm 2.89$	$18.9 \pm 2.16$
$p_T/(2m) > 5$	$0.960 \pm 0.29$	$-1.29 \pm 6.63$	$16.0 \pm 5.11$

**Table:** Fit results for the correlators  $\mathcal{E}_{10;10}$ ,  $c_F^2 \mathcal{B}_{00}$ , and  $\mathcal{E}_{00}$  for the two  $p_T$  regions in the  $\overline{\text{MS}}$  scheme at the scale  $\Lambda = 1.5$  GeV. The SDC  $c_F$  is computed for the charm quark mass  $m = 1.5$  GeV.

The uncertainties in above table are highly correlated and the correlation matrices are

$$C_{p_T/(2m)>3} = \begin{pmatrix} 0.0153 & -0.308 & 0.267 \\ -0.308 & 8.35 & -5.17 \\ 0.267 & -5.17 & 4.68 \end{pmatrix} \text{ GeV}^4, \quad (17a)$$

$$C_{p_T/(2m)>5} = \begin{pmatrix} 0.0846 & -1.68 & 1.48 \\ -1.68 & 44.0 & -28.6 \\ 1.48 & -28.6 & 26.1 \end{pmatrix} \text{ GeV}^4. \quad (17b)$$

## Fitting results in terms of $J/\psi$ LDMEs

$p_T$ region	$\langle \mathcal{O}^{J/\psi}(^3S_1^{[8]}) \rangle$	$\langle \mathcal{O}^{J/\psi}(^1S_0^{[8]}) \rangle$	$\langle \mathcal{O}^{J/\psi}(^3P_0^{[8]}) \rangle / m^2$
$p_T/(2m) > 3$	$1.66 \pm 0.18$	$-3.47 \pm 1.41$	$3.07 \pm 0.35$
$p_T/(2m) > 5$	$1.40 \pm 0.42$	$-0.63 \pm 3.22$	$2.59 \pm 0.83$

**Table:** Numerical results for the  $J/\psi$  color-octet LDMEs in units of  $10^{-2} \text{ GeV}^3$ .

- The large uncertainties for  $p_T^{\text{cut}} = 5 \times 2m$  mainly come from the lack of large  $p_T$  data from  $\Upsilon(nS)$  states and the strong cancellation between  $^3S_1^{[8]}$  and  $^3P_J^{[8]}$  channels at very large  $p_T$ .
- The uncertainties are highly correlated. Usually, for quarkonium related physical observable at the LHC, the uncertainties will be significantly reduced when the correlation matrices are taken into account.

# Compare with LHC production data

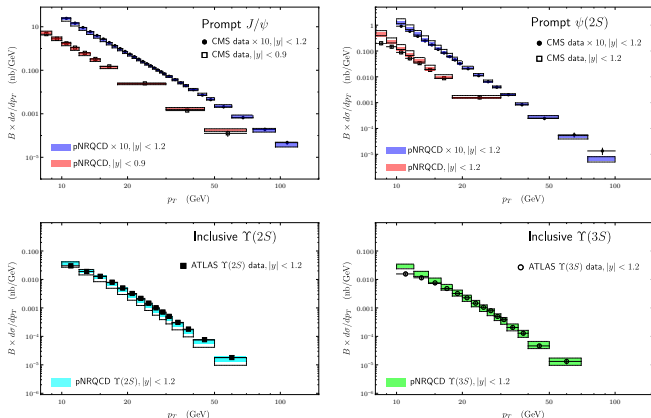


**Figure:** The  $p_T$ -differential cross sections at  $\sqrt{s} = 7$  TeV. For each quarkonium state, the dotted outlined bands are pNRQCD results obtained by excluding that quarkonium data from the fit.

## Compare with existing fittings

	$\langle \mathcal{O}^{J/\psi}(^3S_1^{[8]}) \rangle$	$\langle \mathcal{O}^{J/\psi}(^1S_0^{[8]}) \rangle$	$\langle \mathcal{O}^{J/\psi}(^3P_0^{[8]}) \rangle / m^2$
Hamburg	$0.168 \pm 0.046$	$3.04 \pm 0.35$	$-0.404 \pm 0.072$
ANL	$-0.713 \pm 0.364$	$11 \pm 1.4$	$-0.312 \pm 0.151$
IHEP	$0.117 \pm 0.058$	$5.66 \pm 0.47$	$0.054 \pm 0.005$
PKU set 1	0.05	7.4	0
PKU set 2	1.11	0	1.89
$p_T/(2m) > 3$	$1.66 \pm 0.18$	$-3.47 \pm 1.41$	$3.07 \pm 0.35$
$p_T/(2m) > 5$	$1.40 \pm 0.42$	$-0.63 \pm 3.22$	$2.59 \pm 0.83$

**Table:** Our fitting results and selected existing fitting results for the  $J/\psi$  CO LDMEs in units of  $10^{-2} \text{ GeV}^3$ .

- Our fitting results can be characterized by well constrained positive  $\langle \mathcal{O}^{J/\psi}(^3P_0^{[8]}) \rangle$  and small negative  $\langle \mathcal{O}^{J/\psi}(^1S_0^{[8]}) \rangle$ .

# $\Upsilon(nS)$ polarization predictions

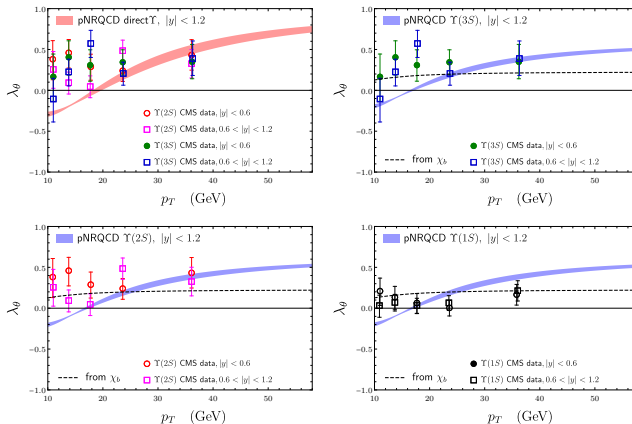


**Figure:** The polarization parameter  $\lambda_\theta$  in the helicity frame compared to CMS measurements ([Chatrchyan \*et al.\*, PRL 110, 081802 \(2013\)](#)). The polarizations of  $\Upsilon$  from  $\chi_b$  decays are shown as black dashed lines.

# $J/\psi, \psi(2S)$ polarization predictions

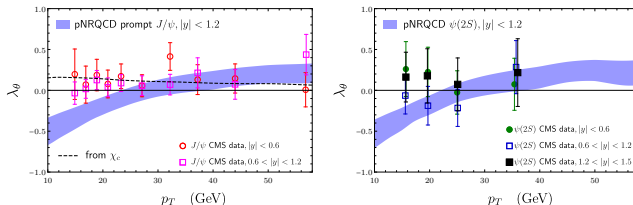


**Figure:** The polarization parameter  $\lambda_\theta$  in the helicity frame for  $J/\psi$  and  $\psi(2S)$  compared to CMS measurements (Chatrchyan *et al.*, PLB 727, 381 (2013)). The polarization of  $J/\psi$  from  $\chi_c$  decays is shown as a black dashed line.

- Our fitting results can simultaneously describe the polarization data of  $\psi(nS)$  and  $\Upsilon(nS)$  reasonably well,
- The  $\Upsilon(nS)$  states are more transversely polarized compared with  $\psi(nS)$  states at comparable values of  $p_T/m$  because  $\mathcal{E}_{00}$  is positive (larger  $\mathcal{E}_{10;10}$  at  $\mu = m_b$ ).

# $\eta_c$ hadron production

- Based on heavy quark spin symmetry:

$$\langle \mathcal{O}_{\eta_c}(^1S_0^{[1]}) \rangle = \frac{1}{3} \langle \mathcal{O}^{J/\psi}(^3S_1^{[1]}) \rangle, \quad \langle \mathcal{O}_{\eta_c}(^3S_1^{[8]}) \rangle = \langle \mathcal{O}^{J/\psi}(^1S_0^{[8]}) \rangle,$$

$$\langle \mathcal{O}_{\eta_c}(^1S_0^{[8]}) \rangle = \frac{1}{3} \langle \mathcal{O}^{J/\psi}(^3S_1^{[8]}) \rangle, \quad \langle \mathcal{O}_{\eta_c}(^1P_1^{[8]}) \rangle = 3 \langle \mathcal{O}^{J/\psi}(^3P_0^{[8]}) \rangle,$$

and our fitting results of  $J/\psi$  LDMEs, we plot our predictions on  $\eta_c$  hadron production cross sections.

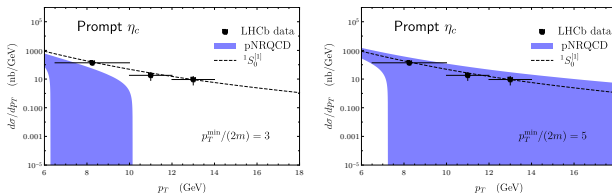
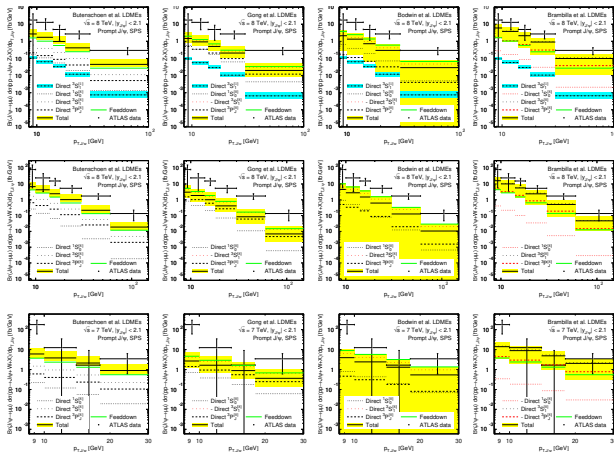


**Figure:** Production rate of  $\eta_c$  at the  $\sqrt{s} = 7$  TeV LHC in the rapidity range  $2.0 < y < 4.5$  compared with LHCb data ([LHCb collaborations, EPJC 68 \(2010\) 401](#)). The color-singlet contribution at leading order in  $v$  is shown as black dashed lines.

# $J/\psi + W/Z$ hadron production



Figures taken from [M. Butenschön, B. Kniehl, arXiv: hep/ph-2207.09366](#).

Our fitting gives better description (see more details from the talk of Mathias.)

# Photoproduction of $J/\psi$

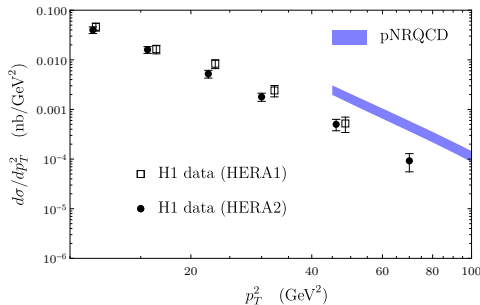


**Figure:** Photoproduction cross section of  $J/\psi$  at HERA compared to H1 data ([H1 collaboration, EPJC 25 \(2002\) 25; EPJC 68 \(2010\) 401](#)).

- Our fitting overshoots the data, which is also a common situation for all the existing large  $p_T$  hadron production fittings.

# $J/\psi$ production at the EIC ( $ep$ rest frame)

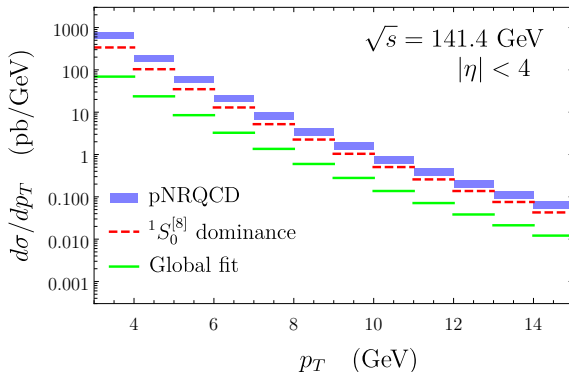


**Figure:** The  $p_T$  differential cross section at the EIC with  $\sqrt{s} = 141.4 \text{ GeV}$  and pseudo-rapidity  $|y| < 4$  in the electron-proton rest frame. The NLO SDCs are taken from [J. Qiu, X.P. Wang, H. Xing, Chin.Phys.Lett. 38 \(2021\) 4, 041201](#)

## Summary & conclusions

- With pNRQCD in the strong coupled region, we have expressed the spin-1  $S$ -wave NRQCD LDMEs in terms of wave-functions at the origin and 3 universal gluonic correlators, which are more amenable in lattice calculations.
- Due to the flavor independence of the gluonic correlators, the number of independent LDMEs are greatly reduced, this brings in a substantial enhancement in the predictive power of the NRQCD factorization.
- Thanks to the evolution of the  $\mathcal{E}_{10;10}$ , we are able to strongly constrain the  $P$ -wave CO LDMEs ( $\mathcal{E}_{00}$ , hence  $\langle \mathcal{O}^{J/\psi}(^3P_0^{[8]}) \rangle$ ), which has not been possible in existing works.
- We expect the sign (positive) of  $\mathcal{E}_{00}$  ( $\langle \mathcal{O}^{J/\psi}(^3P_0^{[8]}) \rangle$ ) will not change due to higher order QCD corrections because radiative corrections shall effect the charmonium and bottomonium SDCs in a similar way at large  $p_T$ .

## Summary & conclusions – continued

- The positive values of  $\langle \mathcal{O}^{J/\psi}(^3P_0^{[8]}) \rangle$  we have obtained are also supported by the polarization data: the  $\Upsilon(nS)$  states are more transversely polarized compared with  $\psi(nS)$  states at comparable value of  $p_T/m$ .
- Our fittings are also favored by  $\eta_c$  hadron production data and  $J/\psi + W/Z$  hadron production data.
- We also give our predictions on inclusive  $J/\psi$   $p_T$  differential cross sections in the electron-proton rest frame at the EIC
- More large  $p_T$  hadron production data of excited  $\Upsilon$  states may help to further reduce the fitting uncertainties.
- It is surprising and exciting that pNRQCD in strong coupled region works so well for the spin-1  $S$ -wave quarkonia, which may indicate a promising direction to pin down the quarkonium production mechanism.